A new method for development of bond-order potentials for transition bcc metals

2014 Modelling Simul. Mater. Sci. Eng. 22 034002

(http://iopscience.iop.org/0965-0393/22/3/034002)

IOP Publishing Modelling and Simulation in Materials Science and Engineering

Modelling Simul. Mater. Sci. Eng. **22** (2014) 034002 (22pp) doi:10.1088/0965-0393/22/3/034002

A new method for development of bond-order potentials for transition bcc metals

Yi-Shen Lin[1], **M Mrovec**[2] **and V Vitek**[1]

[1] Department of Materials Science and Engineering, University of Pennsylvania, Philadelphia, PA 19104, USA
[2] Fraunhofer Institute for Mechanics of Materials IWM, Wöhlerstrasse 11, 79108 Freiburg, Germany

E-mail: vitek@seas.upenn.edu

Received 1 October 2013, revised 4 December 2013
Accepted for publication 10 January 2014
Published 1 April 2014

Abstract

A new development of numerical bond-order potentials (BOPs) for the non-magnetic transition metals V, Nb, Ta, Cr, Mo and W is presented. The principles on which the BOPs have been set up are the same as in earlier developments (Aoki *et al* 2007 *Prog. Mater. Sci.* **52** 154). However, the bond integrals are based on the recently advanced method of parametrization of tight-binding from DFT calculations (Madsen *et al* 2011 *Phys. Rev.* B **83** 4119, Urban *et al* 2011 *Phys. Rev.* B **84** 155119) and do not require any screening. At the same time, the functional form of the environmentally dependent repulsion is identified with the functional form of the repulsion arising from the overlap of s and p electrons in argon as proposed in Aoki and Kurokawa (2007 *J. Phys.: Condens. Matter* **19** 136228). This is justified by the same physical origin of the environment dependent repulsion, which in transition metals arises from the overlap of s electrons that are being squeezed into the ion core regions under the influence of the strong covalent d bonds. The testing of the developed BOPs involves investigation of alternative higher energy structures, transformation paths connecting the bcc structure with other structures via continuously distorted configurations, evaluation of the vacancy formation energy and calculation of phonon spectra. In all cases, the BOP calculations are in more than satisfactory agreement with either DFT calculations and/or available experimental data. The calculated γ-surfaces for $\{1\,0\,1\}$ planes all suggest that the core of $1/2\langle 1\,1\,1\rangle$ screw dislocations is non-degenerate in the transition metals. This is also in full agreement with available calculations that account fully for the quantum-mechanical nature of the d electrons that provide the bulk of the bonding in transition metals. The testing of developed BOPs clearly demonstrates that they are transferable to structures well outside

the regime of the ideal bcc lattice and are suitable for investigating the atomic structure and behaviour of extended crystal defects.

Keywords: transition metals, bond order, environment dependent repulsion, potential testing, potential transferability

(Some figures may appear in colour only in the online journal)

1. Introduction

The precursor of any atomic level modelling of properties of materials is a reliable description of atomic interactions. The present state of the art is the methods based on the density functional theory (DFT) [5–7]. However, in these calculations, the feasible blocks of atoms contain at most a few hundred particles and an even more severe restriction is imposed by the periodic boundary conditions that are required. The latter restriction seriously limits studies of extended crystal defects such as dislocations and interfaces. Consequently, atomic level investigations of large systems without the use of periodic boundary conditions require approximations and simplifications when describing atomic interactions. The most general approach is to coarse-grain the problem, in that the electronic degrees of freedom are removed by imagining the atoms interacting via interatomic potentials [8].

A number of central-force potentials of EAM [9] or Finnis–Sinclair [10] type were developed for transition bcc metals and used in a variety of studies [11–15]. However, in transition metals, the bonding has a mixed nearly free electron and covalent character and it is the filling of the d band that controls the cohesion, and hence the particular ground state structure that a transition metal crystallizes in [16, 17]. The bonding mediated by the d electrons is covalent in character and central force potentials do not reflect this aspect of bonding. This is, presumably, the reason why in studies of the core of $1/2\langle 1\,1\,1\rangle$ screw dislocations different structures and a different response to the applied stress were found when using different potentials for the same metal. Additionally, most of these calculations disagree with studies that explicitly include the electronic structure, in particular DFT calculations (for a review see [18]). This aspect was not improved significantly when directional bonding was included empirically, such that the energy varies with the bond angles when the structure deviates away from the perfect bcc lattice [19, 20]. Hence, it is desirable to include the covalence of bonding that relates to the partially filled d band in a way that is consistent with the quantum character of these bonds (see e.g. [17, 21]).

A scheme that includes the d band mediated directional bonding in transition metals is the many-atom bond-order potentials (BOPs), originally proposed by Pettifor [22]. This scheme gives an accurate representation of the bond energy within the chemically intuitive tight-binding (TB) approximation to the quantum-mechanical electronic structure, and the angular character of the covalent part of the bonding is attained on the fundamental physical basis. It was employed very successfully in a number of atomic level calculations, dislocations in particular [23–26]. The physical basis of BOPs and some of their applications are described in more detail in recent reviews [1,27–29].

Within the BOP scheme, the cohesive energy of non-magnetic transition metals is approximated as the sum of the attractive contribution of the covalent character and repulsive contribution, namely

$$E^{\mathrm{coh}} = E^{\mathrm{cov}} + E^{\mathrm{rep}}. \tag{1}$$

The covalent part of the cohesive energy is written as a sum of the contributions from bonds between individual atoms i and j [27–29]:

$$E^{\mathrm{cov}} = \frac{1}{2}\sum_{i\neq j} E^{\mathrm{cov}}_{i,j}, \tag{2}$$

where

$$E^{\mathrm{cov}}_{i,j} = 2\sum_{\delta,\gamma} H_{i\delta,j\gamma}\Theta_{j\gamma,i\delta}. \tag{3}$$

The indices δ and γ relate to orbitals included in the calculation, and the summation over these indices extends over orbitals associated with the atoms i and j, respectively. $H_{i\delta,j\gamma}$ are the matrix elements of the two-centre TB Hamiltonian, which may be written in terms of the Slater–Koster two-centre bond integrals and direction cosines [30]. $\Theta_{j\gamma,i\delta}$ are the matrix elements of the bond order, the physical meaning of which is half of the difference between the number of electrons in the bonding and antibonding states. The scheme for the evaluation of the bond order was developed by Aoki and Pettifor [1, 31, 32] using inter-site Green's functions, which employ an orthogonal TB basis, two-centre bond integrals and the Lanczos [33] algorithm of continued fractions to calculate the Green's functions [34]. It was found in earlier studies [23, 25, 35] that limiting the continued fractions to nine moments of the density of states reproduces with sufficient precision the main features of the density of states. This number of moments has been used in all of the present calculations. Furthermore, the on-site energies, the diagonal elements of the Hamiltonian, are adjusted self-consistently to guarantee local charge neutrality, which is an excellent approximation for metals [17]. This self-consistent adjustment of the diagonal elements of the Hamiltonian leads to changes in the bond order and thus $E^{\mathrm{cov}}_{i,j}$. A fictitious temperature, T_{f}, is also introduced into the formalism in order to avoid the sharp cut off of the energy at the Fermi level and, consequently, damp down the related long-range Friedel oscillations. This method was introduced by Mermin [36] and is explained in detail for the case of bond order in [37, 38]. This method guarantees a fast convergence of the bond order and related Hellmann–Feynman forces; in our calculations, similar to previous studies, we take $k_{\mathrm{B}}T_{\mathrm{f}}, = 0.3\,\mathrm{eV}$. This method has been implemented in the Oxford order-N package (OXON) [39–42] that has been utilized in both the development and application of BOPs. Apart from the fully quantum-mechanical character, a significant advantage of BOPs is that atomistic modelling can be performed in real space and avoids using the periodic boundary conditions that are necessary in k-space methods.

The most important input needed for evaluation of $E^{\mathrm{cov}}_{i,j}$ (equation (3)) is the bond integrals and their dependence on the distance R_{ij} between the atoms i and j. This is done by fitting the results of DFT-based calculations made for a variety of hypothetical structures of varying densities. In the version used until now, the first-principles TB-LMTO calculations were used for this purpose [43]. In these calculations, the full s, p, d basis was employed and orthogonalized, and then reduced to the d basis only. The corresponding bond integrals of the d type thus contained a contribution from the s and p functions that was manifested for bcc metals and other not-closed packed structures by a marked discontinuity between the distance dependences of the first and second neighbours. In order to ameliorate this problem, screening of bond integrals was introduced [1, 23, 25, 44] that must be evaluated self-consistently during calculations, which contributes very significantly to the computing time needed. In section 2, we introduce a method of evaluating bond integrals in which orthogonalization is performed after reduction to the d basis and the bond integrals need not be screened. This is based on the recently advanced method of the parametrization of TB models from DFT calculations [2, 3].

Within the development of BOPs and any other TB scheme, the attractive part of the energy of the system studied, E^{cov}, is determined fully quantum mechanically without any

empirical input. In contrast, the repulsive part of the energy, E^{rep}, which is equally important in atomistic modelling, is represented by an empirical functional form, the parameters of which are fitted using experiments and/or the results of DFT calculations. In the earlier TB studies, it was commonly assumed that E^{rep} could be described by a pair potential [45, 46]. However, unless the Cauchy pressure, $(C_{12}-C_{44})/2$ in cubic crystals, is determined fully by E^{cov}, the elastic constants cannot be reproduced because the pair potential does not contribute to the Cauchy pressure [47, 48]. Consequently, the repulsive part of the energy has to contain an environment-dependent term, E^{env}, that has a many-body character. The functional form of E^{env} was proposed by Nguyen-Manh [43, 48] to be a screened Yukawa-type potential and this has been employed in all BOPs until now [23–25, 35]. In section 3, we suggest a functional form for E^{env} that is based on the DFT and TB calculations of the energetics of solid argon [4] in which no covalent bonding exists and the term arising from the fully filled shells of s and p electrons is instead repulsive. This form, while still empirical, has some advantages over the Yukawa form and its aptness is demonstrated by testing the developed BOPs.

The BOPs were developed for six non-magnetic transition metals, V, Nb, Ta, Cr[3], Mo and W, which all crystallize in the bcc lattice, and their transferability to different atomic environments was tested. These tests involve comparisons of calculations employing the potentials with those based on DFT. Such calculations include the energetics of several alternative higher energy structures, vacancies and deformation paths [50, 51] which pass through configurations that differ significantly from the ideal bcc lattice and γ-surfaces that relate to the structure of dislocation cores [18]; phonon calculations have also been performed and compared with experiments. The results of these tests suggest that the developed BOPs are capable of capturing the structures and behaviour of extended crystal defects in which atomic configurations differ significantly from the ideal lattice.

2. Attractive part of the cohesive energy and bond integrals

The bond integrals, in particular their dependence on the separation of atoms, are crucial quantities in the BOP scheme since they determine the magnitude of the attractive contribution E^{cov}. In the development presented in this paper, they were obtained directly from DFT calculations via a recently advanced projection scheme [2, 3]. This approach is based on constructing a minimal basis of optimized atomic orbitals (AOs) that give the best possible representation of the electronic wave functions obtained in self-consistent DFT calculations for selected bulk structures representing various geometrical arrangements and bonding environments. The main advantage of this procedure is that it avoids empirical fitting and instead provides a consistent, physically based set of parameters whose validity and range of applicability are known.

In the case of bcc transition metals, the minimal spd AOs basis was first optimized for the bcc phase at its equilibrium volume and then used without further modification for projections in other bulk phases at different volumes. Orbitals optimized just for the equilibrium bcc phase also provide an excellent description of the electronic structure of other phases with very different bonding environments. As an example, this is demonstrated in figure 1, which shows the band structure plots for Mo in three different phases, namely bcc, fcc and simple cubic (sc). The optimized AOs obtained by the projection are orthogonal when they are centred on the same atom but nonorthogonal for centres at different atomic sites. Since the

[3] While Cr is antiferromagnetic, it was shown in [49] using a DFT method that both the non-magnetic and antiferromagnetic phases are BCC with almost identical lattice parameters. Hence, potentials for analyses of structural aspects can be developed assuming a non-magnetic state.

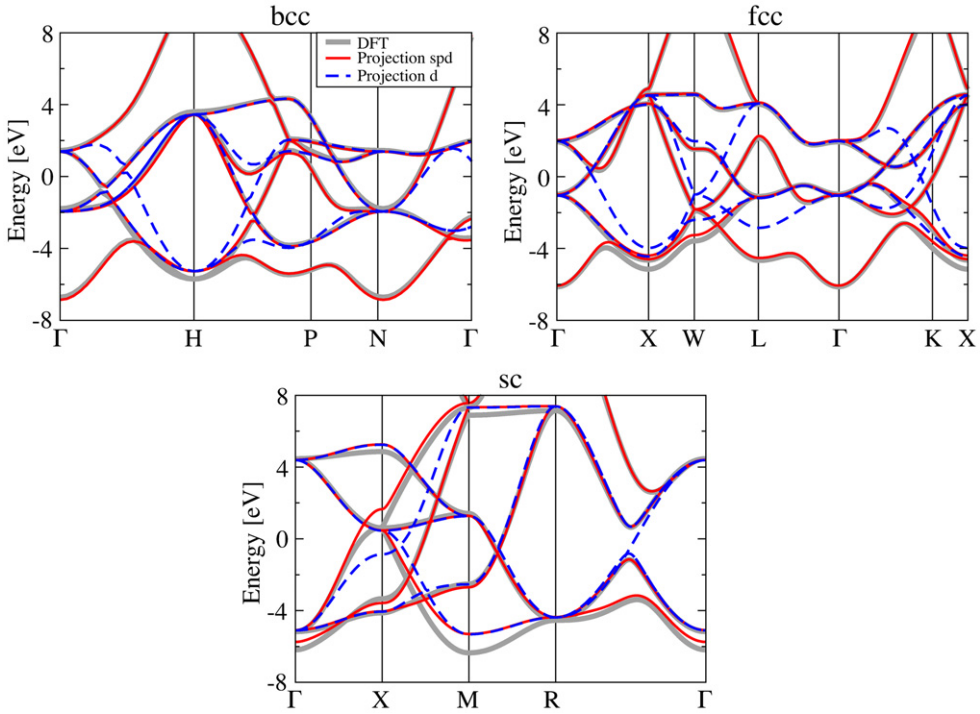

Figure 1. Comparison of band structures for three bulk phases of Mo calculated using the DFT, projected spd and d-only TB models.

BOP formalism is based on the orthogonal TB, it is necessary to obtain appropriate bond integrals that correspond to the orthogonal AOs. The orthogonalization of the AOs basis was carried out using Löwdin's symmetrical orthogonalization [52], which produces orthogonal functions that have the same symmetry as the original nonorthogonal functions and that are also least distorted in the least-square sense. However, as with all orthogonalization procedures, the Löwdin orthogonalization is environment dependent, i.e. the magnitudes, ranges and atomic separation dependences of the resulting orthogonal bond integrals depend not only on the nonorthogonal Hamiltonian and overlap matrix elements but also on the geometry of the particular atomic configuration.

Additionally, in the case of middle transition metals with a partially filled d band, it is possible to reduce the minimal spd to a d-only AOs basis in order to retain just those orbitals that contribute most to the chemical bonding. This reduction results in BOP models that are still able to capture the key essence of chemical bonding while being computationally most efficient. This is again visible in figure 1 where the band structures calculated using DFT, spd projected and d-only projected AOs are presented. However, when only the d AOs are employed, it is necessary to consider whether the orthogonalization is done before or after the reduction of the AOs basis. In simple terms, the orthogonal orbitals are mixtures (linear combinations) of the original orbitals and some orbitals located on the neighbouring atoms. If the full spd basis is kept, then the orthogonal orbitals are admixtures of all three orbital types and, consequently, the corresponding bond integrals are more affected by their surroundings; if the basis is reduced before orthogonalizsation, then the environment dependence of the resulting Hamiltonian elements is weaker.

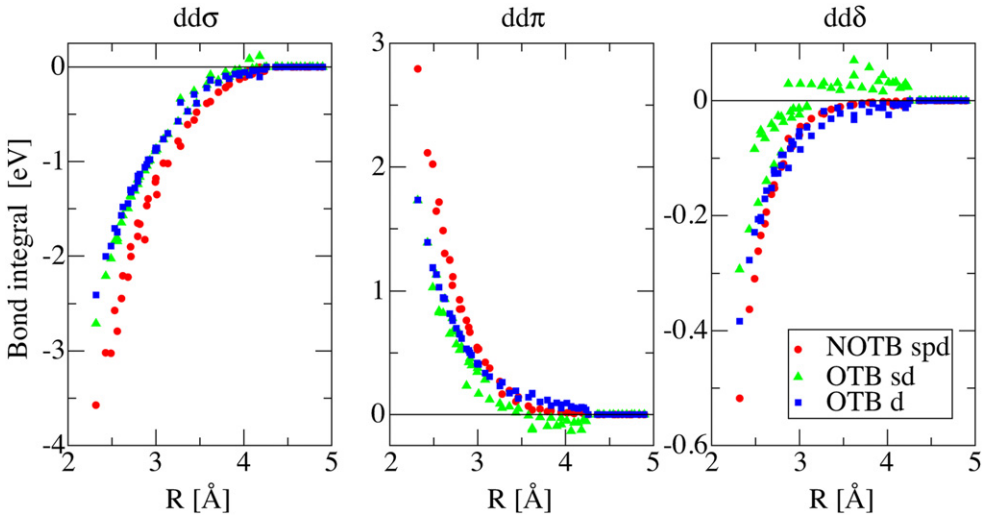

Figure 2. Dependences of ddσ, ddπ and ddδ bond integrals in Mo on the interatomic distance, R, for non-orthogonal (NOTB) and orthogonal (OTB) atomic orbitals; for the latter, only the cases of sd orbitals and d orbitals are shown.

A comparison of the dd type bond integrals for Mo obtained for non-orthogonal AOs with corresponding integrals obtained using an orthogonalized completely reduced d-only and a partly reduced sd basis is shown in figure 2. In both cases, the orthogonalization leads to smaller absolute values of the bond integrals and somewhat increases the range of the interactions. For the partly reduced sd basis the screening effects of the s orbitals are visible for the ddπ and ddδ bond integrals. In this case, the s orbitals contribute significantly to the screening of the interatomic bonds and cause stronger environmental effects, with some of the values that correspond to more distant neighbours even changing their sign [44]. When the completely reduced d-only basis is used, the environmental dependence of all three ddσ, ddπ and ddδ bond integrals is very weak. They can be represented very well by simple continuous functions, which depend on the interatomic distance only. Hence, orthogonalization does not cause any overall decrease in the transferability of bond integrals, and environmental effects need to be considered only when more complete AOs bases are employed.

Elements of groups 5 and 6 comprise five and six valence electrons, respectively. These are distributed between the nearly-free-electron sp band and the TB d band. The number of d electrons, N_{d}, is usually a non-integer due to hybridization and the exact value of N_{d} cannot be determined unequivocally. However, it was shown in [24], using the *ab initio* linear muffin-tin method combined with a frozen potential approximation resolved into the contribution from the d band, that bcc is strongly favoured over the fcc and hcp structures when $3.5 \leqslant N_{\mathrm{d}} \leqslant 4.5$. Hence, we require N_{d} to be in this range and we used $N_{\mathrm{d}} = 3.6$ for group 5 metals and $N_{\mathrm{d}} = 4.2$ for group 6 metals, respectively. The susceptibility of constructed BOPs to the choice of N_{d} was tested by varying N_{d} by ± 0.2 and it was found that potentials employing these various values of N_{d} lead to virtually the same results in all the tests. Hence, the BOPs are insensitive to the details of the choice of N_{d}, provided that it is in a reasonable range. Nevertheless, N_{d} could be used as a fitting parameter if there is a material property that appears to depend markedly on N_{d}.

The d bond integrals based on the orthogonal d-only basis of AOs are displayed for all six bcc transition metals studied as functions of interatomic distance in figure 3. They are

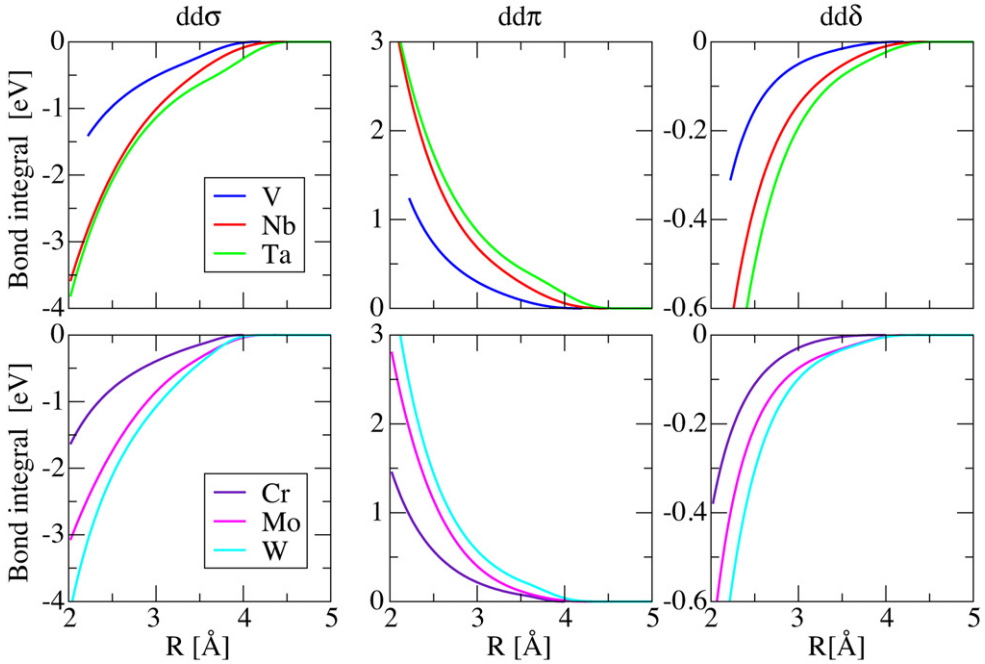

Figure 3. Dependence of the d-only based bond integrals on the separation of atoms for the six transition metals for which BOPs were developed.

represented well by smooth continuous functions of interatomic distance only. We adopt the functional form proposed by Goodwin, Skinner and Pettifor (GSP) [53] to represent them analytically:

$$\mathrm{dd}\tau(R) = \mathrm{dd}\tau_0 \left(\frac{R_0}{R}\right)^{n_\mathrm{a}} \exp\left\{n_\mathrm{a}\left[\left(\frac{R_0}{R_\mathrm{c}}\right)^{n_\mathrm{c}} - \left(\frac{R}{R_\mathrm{c}}\right)^{n_\mathrm{c}}\right]\right\}, \tag{4}$$

where τ represents σ, π and δ, respectively; $\mathrm{dd}\tau_0$, R_0, R_c, n_a and n_c are for the given τ parameters, fitted so as to reproduce the numerically calculated dependences of bond integrals shown in figure 3. The values of these parameters are summarized in table 1.

When employing BOPs in atomistic modelling, it is important for numerical reasons that BOPs go smoothly to zero at a cut off distance so that no discontinuities occur either in energy or forces. In order to achieve this, the bond integrals have to approach zero smoothly at a cut off, $R^{\mathrm{BI}}_{\mathrm{cut}}$, and for this purpose the GSP function is replaced by a fifth-order polynomial tail function between a chosen value R^{BI}_1 and $R^{\mathrm{BI}}_{\mathrm{cut}}$, similar to [23, 25]. The polynomial coefficients are determined so that the polynomial and the GSP functions, as well as their first and second derivatives, are continuous at the joining point R^{BI}_1, and that the value of the polynomial and its first and second derivatives become zero at $R^{\mathrm{BI}}_{\mathrm{cut}}$. In order to limit the range of the interactions, the cut off distance, $R^{\mathrm{BI}}_{\mathrm{cut}}$, was chosen to be between the second and third neighbours for all bcc metals studied; the values of R^{BI}_1 and $R^{\mathrm{BI}}_{\mathrm{cut}}$ are listed in table 2.

3. Repulsive part of the cohesive energy

As alluded to in section 1, the repulsive part of the cohesive energy cannot be derived rigorously quantum mechanically as the attractive covalent part is. Instead, a physically justified empirical

Table 1. Parameters used in equation (4) when R is in Å.

	Vanadium				Chromium		
	ddσ	ddπ	ddδ		ddσ	ddπ	ddδ
ddτ_0 (eV)	−0.8274	0.5841	−0.1149	ddτ_0 (eV)	−0.8093	0.5751	−0.1121
R_0 (Å)	2.6240	2.6240	2.6240	R_0 (Å)	2.4942	2.4942	2.4942
R_c (Å)	4.3513	4.2725	4.7363	R_c (Å)	4.1299	4.7377	4.0634
n_a	3.0841	4.3400	5.8900	n_a	3.2481	3.5214	5.3773
n_c	9.6280	9.9998	9.9999	n_c	9.7642	3.5653	8.0456
	Niobium				Molybdenum		
	ddσ	ddπ	ddδ		ddσ	ddπ	ddδ
ddτ_0 (eV)	−1.3032	0.9128	−0.1989	ddτ_0 (eV)	−1.2858	0.7211	−0.1278
R_0 (Å)	2.8172	2.8172	2.8172	R_0 (Å)	2.7256	2.7256	2.7256
R_c (Å)	2.9105	2.9105	2.9105	R_c (Å)	3.0151	3.1861	9.1897
n_a	1.2251	1.9838	2.4495	n_a	1.1771	2.0492	5.5827
n_c	2.2892	1.3182	1.2273	n_c	3.0793	2.7101	8.7383
	Tantalum				Tungsten		
	ddσ	ddπ	ddδ		ddσ	ddπ	ddδ
ddτ_0 (eV)	−1.3390	1.0477	−0.2493	ddτ_0 (eV)	−1.5390	0.9183	−0.1755
R_0 (Å)	2.8629	2.8629	2.8629	R_0 (Å)	2.7411	2.7411	2.7411
R_c (Å)	1.3776	1.0155	1.1710	R_c (Å)	4.1519	1.0895	1.0000
n_a	1.0000	1.0000	1.4194	n_a	3.0486	1.3041	1.6529
n_c	1.0882	1.0155	1.0754	n_c	9.5003	1.0729	1.0000

Table 2. R_1^{BI} and $R_{\mathrm{cut}}^{\mathrm{BI}}$ in units of the lattice parameters for the metals studied.

	V	Nb	Ta	Cr	Mo	W
R_1^{BI}	1.053	0.909	1.059	1.040	1.049	1.106
$R_{\mathrm{cut}}^{\mathrm{BI}}$	1.382	1.363	1.391	1.387	1.366	1.390

formula needs to be found and adjusted such that the dependence of E^{coh} on the relative positions of particles can reproduce either the experimental or DFT calculated basic properties of the metal under study. As in the earlier version of BOPs [1, 23, 25], we write

$$E^{\mathrm{rep}} = E^{\mathrm{env}} + E^{\mathrm{pair}}, \tag{5}$$

where E^{pair} is the contribution described by a pair potential and E^{env} is the environment dependent repulsion. The latter is a function of the separations of particles, but owing to the many-body character of the interactions it implicitly contains the dependence on bond angles. In BOPs developed until now [1, 23–25, 35], E^{env} takes the form of a screened Yukawa-type potential. This form, proposed by Nguyen-Manh [43, 48], was deduced from calculations that employed the Harris–Foulkes method of extracting TB models from DFT [54, 55]. This form of E^{env} was used in BOPs for Mo and W [23, 25] that successfully described a number of properties of these metals, in particular the core structure of the screw dislocations and its response to the applied stress tensor [26, 56, 57]. However, in some other bcc transition metals, the very rapid increase in the Yukawa-type potential with the decreasing separation of particles (e.g. Nb and Ta) led to problems that prompted us to search for a different form of

E^{env} [58]. Moreover, the physical reason for the functional form of E^{env} employed in this paper is more transparent than in the case of the Yukawa-type form, although there is no fundamental reason why the Yukawa-type function cannot be used to represent the environment dependent repulsion.

Recently, Aoki and Kurokawa [4] studied the environment dependent repulsion arising from the overlap of s and p closed-shell electrons in the solid argon. Using the non-orthogonal TB bond model [5, 46], they calculated E^{cov}, which is always environment dependent but which in this case represents the overlap repulsion rather than attraction since in argon the 3s and 3p shells are fully occupied. On this basis they suggested the following form for the overlap repulsion:

$$E^{\text{env}} = \frac{1}{2}\sum_{i,j\neq i} V(R_{ij})\mathrm{e}^{-(\lambda_i+\lambda_j)R_{ij}}, \tag{6a}$$

where

$$\lambda_i = \sum_{i\neq k} g\exp(-\nu R_{ik}) \tag{6b}$$

and g and ν are adjustable parameters. The environmental effect is hidden in λ_i and λ_j, on which E^{env} depends exponentially, similar to the Yukawa-type potential. $V(R_{ij})$ is an environmentally independent pairwise function, which was proposed in [4] to be taken as a polynomial multiplied by an exponential rapidly decaying with increasing R_{ij} (see equation (37) of [4]). Using this model of overlap repulsion, supplemented by a van der Waals pairwise attraction, Aoki and Kurokawa [4] showed excellent agreement with an experimentally measured dependence of the lattice parameter and elastic constants of fcc argon on applied external pressure. In particular, the environmental dependence of the repulsion leads to the correct Cauchy pressure, which would be zero if only pairwise interactions were present.

Our conjecture is that the functional form of E^{env}, given by equations (6*a*) and (6*b*), is not only an excellent description of environmentally dependent repulsion for solid argon but also a useful form for the description of E^{env} in transition metals. The reason is that in these metals, the environment dependent repulsion also arises from the overlap of s electrons that are being squeezed into the ion core regions under the influence of the large covalent d-bonding forces [59]. For the function $V(R_{ij})$ we only include the exponential dependence on R_{ij}

$$V(R_{ij}) = A\exp(-\mu R_{ij}), \tag{7}$$

replacing the polynomial function suggested in [4] by a constant A. For E^{env} we take a slightly modified equation (6*a*), mainly

$$E^{\text{env}} = \frac{1}{2}\sum_{i,j\neq i} V(R_{ij})\mathrm{e}^{-(\lambda_i+\lambda_j)(R_{ij}-R_s)}. \tag{8}$$

The introduction of the constant R_s, similar to the case of the Yukawa form, assures that the exponential term rapidly increases with decreasing R_{ij}, leading to a strong repulsion for very small separations of atoms. In this scheme, there are five adjustable parameters: g, ν, A, μ and R_s. The pairwise interaction is

$$E^{\text{pair}} = \frac{1}{2}\sum_{i,j\neq i} \Phi(R_{ij}), \tag{9a}$$

where Φ is a pair potential taken in the form of a cubic spline as in the previous developments of the BOPs:

$$\Phi(R_{ij}) = \sum_{k=0}^{4} B_k(R_k - R_{ij})^3 H(R_k - R_{ij}). \tag{9b}$$

Table 3. Cohesive energies, E_{coh}, lattice parameters a and elastic moduli (in 10^{11} Pa) for the six metals considered. Values of E_{coh} are taken from [64] and elastic moduli from [65] (see also [10]).

	V	Nb	Ta	Cr	Mo	W
E_{coh} (eV)	5.31	7.57	8.10	4.10	6.82	8.90
C_{11}	2.279	2.466	2.660	3.871	4.647	5.224
C_{12}	1.187	1.332	1.612	1.035	1.615	2.044
C_{44}	0.426	0.281	0.824	1.008	1.089	1.606
a (Å)	3.0399	3.3008	3.3058	2.8845	3.1472	3.1652

Table 4. Parameters of the environment dependent repulsion given by equations (6*b*), (7) and (8) when R_{ij} is in units of the lattice parameter a. For all six metals $R_s = 0.52$ (in units of a); μ, g and ν are dimensionless.

	V	Nb	Ta	Cr	Mo	W
A (eV)	1.633×10^4	1.841×10^4	1.870×10^4	4.036×10^2	2.233×10^4	2.537×10^4
μ	13.0	13.0	13.0	7.0	13.0	13.0
g	100.0	300.0	300.0	20.0	300.0	300.0
ν	10.0	10.0	10.0	6.0	10.0	10.0

B_k and R_k are adjustable parameters and H is the Heaviside step function; R_4 is the value of the cut off of the pair potential.

Parameters occurring in both the environment dependent repulsion, entering equations (6*b*), (7) and (8), and the pairwise interaction, given by equation (9*b*), are determined so as to reproduce the lattice parameter, cohesive energy and three elastic constants C_{11}, C_{12} and C_{44} for the equilibrium bcc structure of the metal studied. The experimental data are summarized in table 3, the parameters of the environment dependent repulsion are summarized in table 4 and the pair potential is summarized in table 5. Moreover, B_0 and R_0 are fitted so as to reproduce the dependence of E^{coh} on the decreasing lattice parameter for the gradually compressed bcc lattice that has been calculated independently using DFT as implemented in the VASP code [60–63]. Figure 4 shows that the dependence of E^{coh} on the decreasing lattice parameter calculated by BOPs reproduces the DFT calculations very closely. This ensures that the repulsion for the separation of atoms that is considerably smaller than the first nearest neighbour spacing is well described by BOPs.

The dependence of the pair potential Φ on the separation of particles, R, is shown for the six bcc metals considered in figure 5. This potential is strongly repulsive for separations of atoms considerably smaller than the first nearest neighbour spacing. This is achieved by choosing R_0 in equation (9*b*) to be smaller than the separation of the first nearest neighbours. Figure 5 also shows that the pair potential is weakly attractive between the second and third neighbours of the bcc lattice. This attraction can be regarded as arising from the interaction of s electrons and the sd hybridization at atoms separated at distances close to the second neighbours. The same small attractive part of the pair potential was also found in the previous developments of BOPs [23, 25].

Finally, with the increasing separation of atoms all of the interactions rapidly decrease and can be regarded as negligible beyond a cut off, R_{cut}^{rep}, which is positioned close to the third neighbours of the bcc lattice. In order to achieve a smooth cut off of BOPs, $g\exp(-\nu R)$ in equation (6*b*) and $V(R)$ in equation (7) are replaced by fifth-order polynomials in the range

Table 5. Parameters of the pair potential Φ given by equation (9*b*). Units of R_k are Å and B_keV Å^{-3}. R_0 is in all cases taken to be 0.9 of the nearest neighbour spacing in the equilibrium bcc lattice. R_{ij} have to be given in Å when using the above values of R_k and B_k.

	V		Nb		Ta	
k	R_k	B_k	R_k	B_k	R_k	B_k
0	2.37	10.0	2.57	14.0	2.58	3.0
1	3.00	1.778 777 68	3.30	2.940 866 97	3.00	−1.741 168 99
2	3.10	−0.873 072 91	3.40	−1.525 327 55	3.10	4.193 795 00
3	4.00	1.128 958 69	4.40	1.723 222 67	4.45	1.275 295 81
4	4.20	−0.675 111 31	4.60	−1.085 079 50	4.60	−0.831 521 38
	Cr		Mo		W	
	R_k	B_k	R_k	B_k	R_k	B_k
0	2.25	14.0	2.45	12.0	2.47	15.0
1	2.60	6.369 232 68	3.10	1.508 753 26	2.80	1.607 810 48
2	2.70	−0.626 651 52	3.60	0.925 974 11	3.15	2.752 143 67
3	3.50	1.105 005 82	4.20	1.170 332 76	4.10	1.287 647 84
4	4.00	−0.224 261 97	4.30	−0.972 243 21	4.40	−0.589 211 66

$R_1^{\text{rep}} < R < R_{\text{cut}}^{\text{rep}}$, such that their values, first derivatives and second derivatives are continuous at $R = R_1^{\text{rep}}$ and zero at the cut off $R_{\text{cut}}^{\text{rep}}$. Similar to the case of bond integrals, this modification has been introduced for numerical reasons when employing BOPs in atomistic modelling so that no discontinuities occur either in energy or forces. With the exception of Nb, the values of R_1^{rep} and $R_{\text{cut}}^{\text{rep}}$ are taken to be the same as the corresponding values defining the cut off of the bond integrals, so that $R_1^{\text{rep}} = R_1^{\text{BI}}$ and $R_{\text{cut}}^{\text{rep}} = R_{\text{cut}}^{\text{BI}}$ (see table 2). Moreover, the values of R_4 that determine the cut off of the pair potential (equation (9*b*)) are equal to $R_{\text{cut}}^{\text{rep}}$. Hence, the range of the repulsion is the same as that of attraction. However, for Nb $R_{\text{cut}}^{\text{rep}}$ is still the same as $R_{\text{cut}}^{\text{BI}}$ $(1.363a)$ but $R_1^{\text{rep}} = 1.060a$ and $R_4 = 1.394a$, so that the cut off of the pair potential is about 2% larger than the corresponding $R_{\text{cut}}^{\text{BI}}$.

4. Testing of the developed BOPs

The reason for the development of BOPs is their use in computer modelling of crystal defects, most importantly extended defects such as dislocations, grain boundaries and other interfaces, cracks etc, as well as interactions between the defects. Obviously, some unphysical structural instabilities or metastable configurations must not occur in the cores of such defects when using BOPs. Hence, it is essential that the potentials are capable of adequately describing interactions between the atoms in environments that differ significantly from the equilibrium bcc structure, the properties of which are the main input for their development. While this can never be guaranteed absolutely, the transferability of the potentials needs to be thoroughly tested before they can be employed with confidence in studies of defects that control the behaviour of materials. Naturally, the testing cannot be made for any configuration that may be encountered in atomic level calculations, but several different studies that involve atomic environments that differ significantly from the ideal bcc lattice enhance the confidence in the potentials. In this paper, testing has been performed by investigating alternative crystal structures, determining formation energies of vacancies, calculation of γ-surfaces [18, 66] for

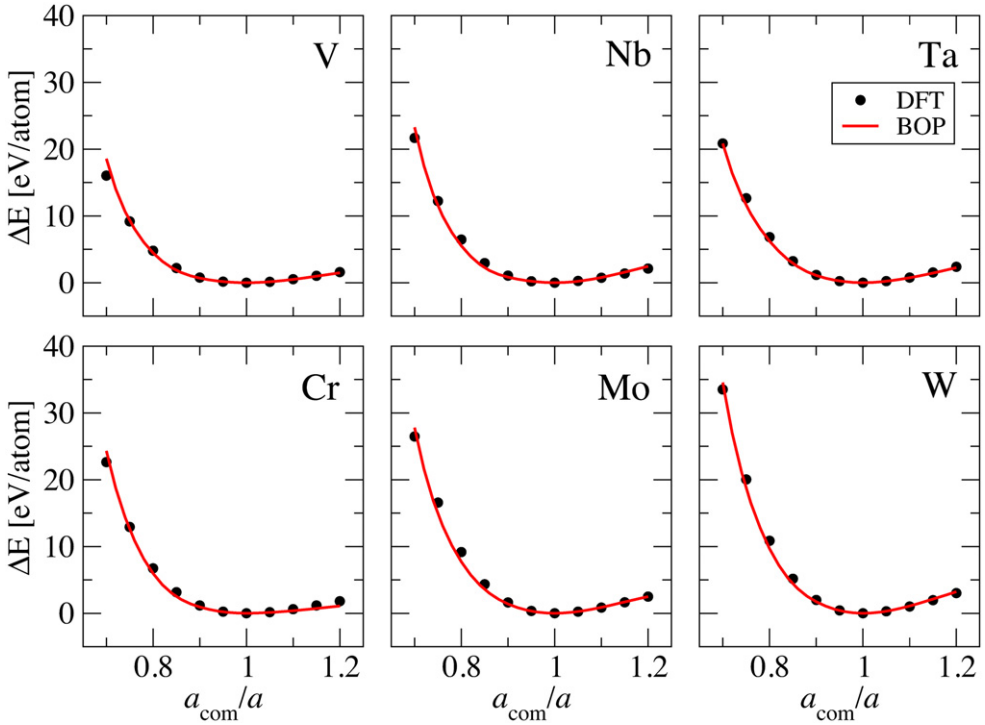

Figure 4. Dependence of the difference between the energy of hydrostatically compressed bcc lattice and that of ideal bcc lattice, ΔE, on the ratio a_{com}/a, where a_{com} is the lattice parameter of the compressed bcc lattice.

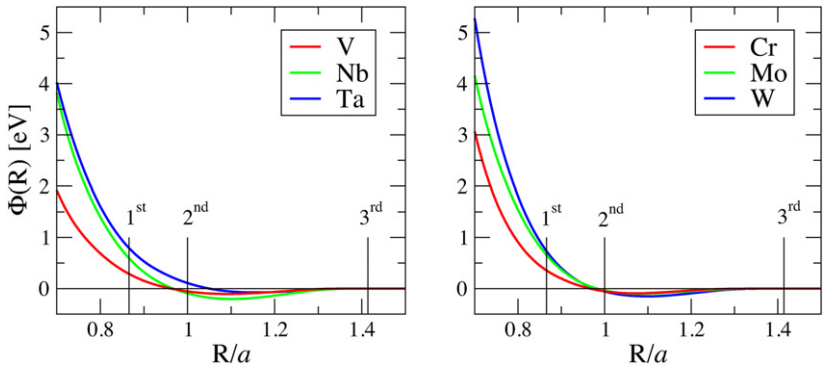

Figure 5. Dependence of the pair potential Φ on the separation of atoms R. The vertical lines denoted as 1st, 2nd and 3rd mark the separations of the first, second and third nearest neighbours in the equilibrium bcc lattice.

{1 0 1} planes and evaluating energy variation when deforming the material following several transformation paths. In all of these cases, the calculations performed using BOPs can be directly compared with DFT-based calculations that were performed using the VASP code [61–63, 67] and in the case of vacancies also with experiments. Another important test is the calculation of the phonon spectra that can be compared with experiments.

Table 6. Energies (meV/atom) of the four relaxed alternate structures measured relative to the energy of the bcc lattice calculated using the constructed BOPs and a DFT method (VASP), respectively.

	V		Nb		Ta		Cr		Mo		W	
	DFT	BOP	DFT	BOP	DFT	BOP	DFT	BOP	DFT	BOP	DFT	BOP
A15	46	66	105	94	24	109	65	157	90	231	84	286
fcc	243	241	324	336	247	280	389	374	425	423	495	492
hcp	287	288	350	422	330	445	447	397	472	448	577	551
sc	848	668	991	991	1105	1165	1019	1042	1087	1400	1433	1841

Table 7. Vacancy formation energies (eV) calculated using BOPs, DFT and measured experimentally.

	V	Nb	Ta	Cr	Mo	W
BOP	2.19	3.37	3.23	2.46	2.88	4.10
DFT	2.51	2.99	3.14	2.64	2.96	3.56
Experiment	2.1–2.2	2.6–3.1	2.8–3.1	2.0–2.4	2.6–3.2	3.5–4.1

4.1. Alternative structures

The alternative structures that were investigated are A15, fcc, hcp and simple cubic (sc). In all of these cases the structures were relaxed, minimizing their energy with respect to the corresponding lattice parameter. The results of this study are presented in table 6.

In all of the cases, the energy difference increases from the A15 structure to the simple cubic structure, which is well reproduced by BOPs. For fcc, hcp and sc the energy differences calculated by BOPs reproduce those calculated by DFT within about 20%. However, the difference between the DFT and BOP calculations is often much larger for the A15 structure. This is a known problem encountered in TB schemes [68], the origin of which is not well understood. It is possible that the proximity of some atoms in the A15 structure may lead to a significant local change in the density of electrons, which cannot be captured by BOPs.

4.2. Vacancy formation energies

The calculations of vacancy formation energies by BOPs were performed using supercells with the dimensions $3a \times 3a \times 3a$ and periodic boundary conditions. The local atomic relaxation was carried out but no change in the volume of the cell was allowed. The results of this calculation are presented in table 7 together with experimentally measured formation energies [69] and those evaluated in [70] using a DFT method and similar supercells and atomic relaxations. Calculations using BOPs are in good agreement with both DFT calculations and experiments.

4.3. Transformation paths

The transformation paths investigated connect the bcc structure with fcc, sc and hcp structures via continuously distorted configurations. Some paths also pass through a body centred tetragonal structure (bct). The volume per atom remains fixed in all the paths. The most common is the tetragonal path, also known as the Bain path [71]. Starting from the bcc lattice and selecting the [0 0 1] direction as the c-axis, this path corresponds to the continuous variation of the c/a ratio, where a is the lattice parameter in the [1 0 0] and [0 1 0] directions.

Such deformation is fully described by the parameter $p = c/a$, which is equal to 1 for the bcc lattice and $\sqrt{2}$ for the fcc lattice.

The next path, trigonal, concurs with the homogeneous deformation corresponding to the extension along the [1 1 1] axis while keeping the atomic volume constant. This path connects three cubic structures, bcc, sc and fcc and can again be described by one parameter p that varies from 1 for bcc, through 2 for sc to 4 for fcc lattices. Both of these paths can be expressed rigorously via a Lagrange strain tensor as described in [50].

The orthorhombic path, which was not considered in [50], connects two bcc structures using a symmetry-dictated maximum that corresponds to a bct lattice. In the coordinate system with the axis $x = [1\,1\,0]$, $y = [\bar{1}\,1\,0]$ and $z = [0\,0\,1]$, it corresponds to elongation in the [0 0 1] direction and simultaneous compression in the [1 1 0] direction. This can again be described by one parameter, p, that enters the corresponding Lagrange strain tensor, which has in the above axes two non-zero components

$$\varepsilon_{11} = (p^{-1} - 1)/2 \qquad \varepsilon_{33} = (p - 1)/2. \tag{10}$$

$p = 1$ and $p = 2$ correspond to the bcc structures and $p = \sqrt{2}$ to the bct structure.

Finally, the hexagonal path connects the bcc and hcp lattices and differs qualitatively from the other paths since it does not correspond only to a homogeneous deformation. Instead, it is a combination of a homogeneous deformation that preserves the atomic volume, with shuffling of alternate close packed atomic planes in the opposite directions. It can again be characterized by one parameter p that enters both the homogeneous straining and shuffling, which are linearly coupled. The details of this complex mode of transformation are described in [50]; $p = 1$ corresponds to the bcc lattice and $p = \sqrt{2}$ to the hcp lattice while the other structures encountered along this path are orthorhombic.

The energy of the structures developing along the transformation paths was evaluated as a function of the parameter p for the six metals studied using both the developed BOPs and the DFT employing the VASP code. A comparison of the two types of atomistic calculations is illustrated in figure 6, which shows an excellent agreement between the BOPs and DFT calculations. Only in the vicinity of the sc structure do the two calculations deviate more significantly for some cases. Similar to the A15 structure, in the sc structure some atoms are appreciably closer to each other than the first nearest neighbours in the bcc lattice and this may lead to a local change in the electronic structure that cannot be captured by BOPs.

4.4. Phonons

The phonon dispersion curves were calculated for the equilibrium bcc structure using the method of frozen phonons [72]. The results of these calculations are compared with experimental observations in figure 7. The calculated longitudinal mode (L) is represented by black curves, transversal modes (T or T1) by red curves and transversal mode T2 by the green curve. Experimental data are depicted by dots using the same colours for the corresponding modes as above. A comparison of the calculations with experiments demonstrates that the BOPs are able to describe well the vibrational behaviour with only some discrepancies at zone boundaries. In particular, anomalies observed for V, Nb, Ta and Cr between Γ and H are not reproduced adequately. These anomalies were discussed in the framework of the TB in [73] and, presumably, the limitation to nine moments of the density of states is not sufficient for capturing these features of the phonon spectra. Nevertheless, these results confirm the robustness of the model since no information about the phonon spectra has been included in the fitting database.

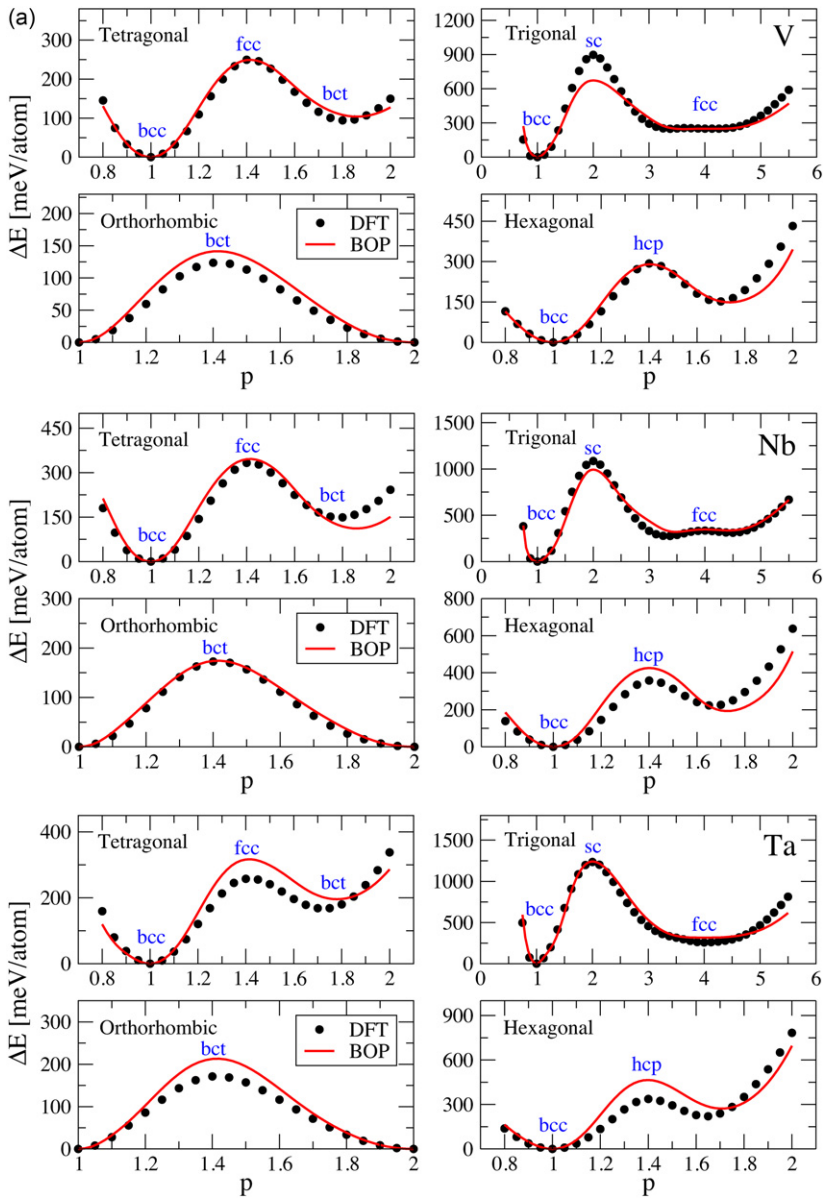

Figure 6. Energy of the structures developing along four transformation paths, measured relative to that of the equilibrium bcc lattice. (*a*) Group V metals. (*b*) Group VI metals.

4.5. γ-surfaces and cores of $1/2\langle 1\,1\,1\rangle$ screw dislocations

It has now been firmly established that the principal characteristics of the plastic deformation of single crystals of bcc metals are governed by $1/2\langle 1\,1\,1\rangle$ screw dislocations that possess non-planar cores (for reviews see [18, 80]). In this section, we show that the constructed BOPs lead to the same basic characteristics of the cores of these dislocations as those established in recent DFT studies [81–85]. The most important features of dislocation cores can be investigated

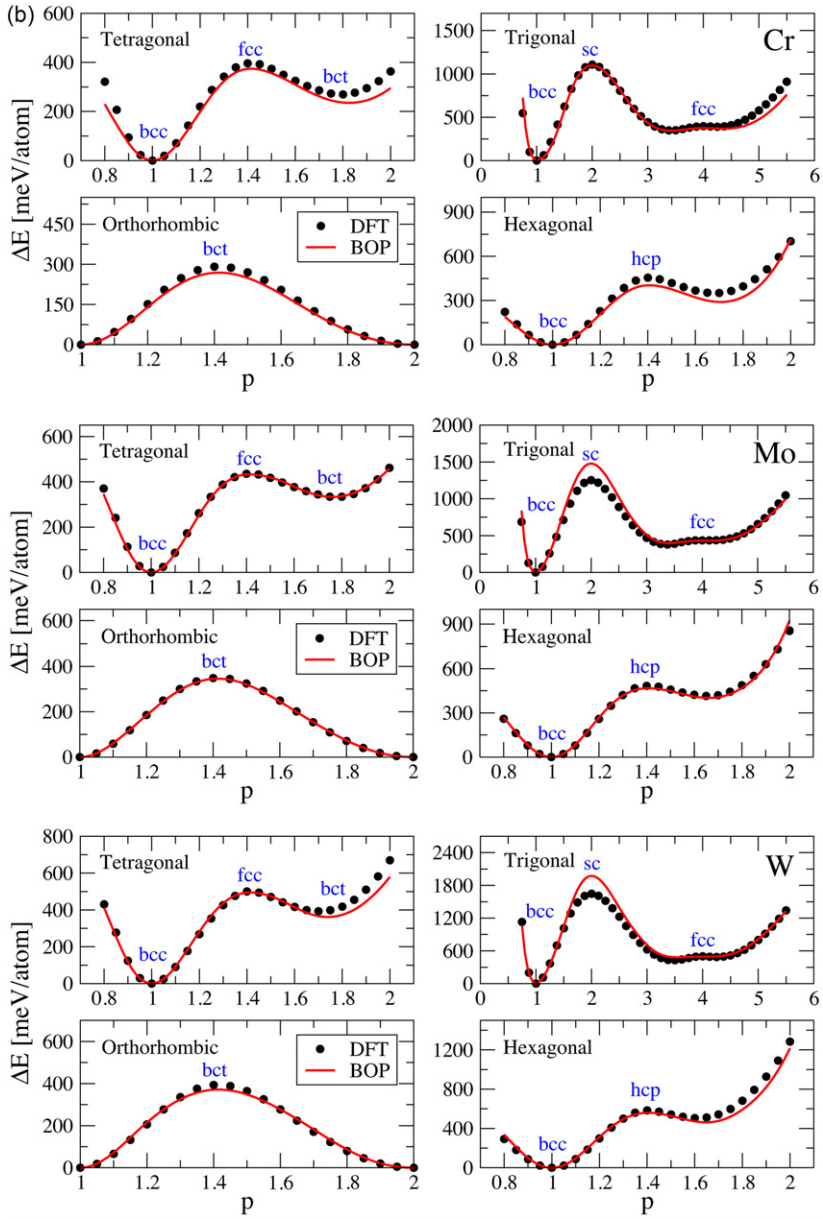

Figure 6. Continued.

using the concept of γ-surfaces introduced in [66]. Such surfaces are determined by calculating the energies of generalized single layer stacking faults formed by displacing relative to each other two parts of a crystal cut along a crystallographic plane. Local minima on these surfaces resolve the displacement vectors of all the possible metastable single layer stacking faults, which then determine the potential dislocation dissociations that are the major characteristic of the atomic level structure of dislocations. Many calculations of γ-surfaces, ranging from pair potentials to DFT-based studies, were performed for the $\{1\,0\,1\}$ and $\{1\,1\,2\}$ planes in bcc crystals and none of them show any metastable stacking faults [18, 80]. As an example, in

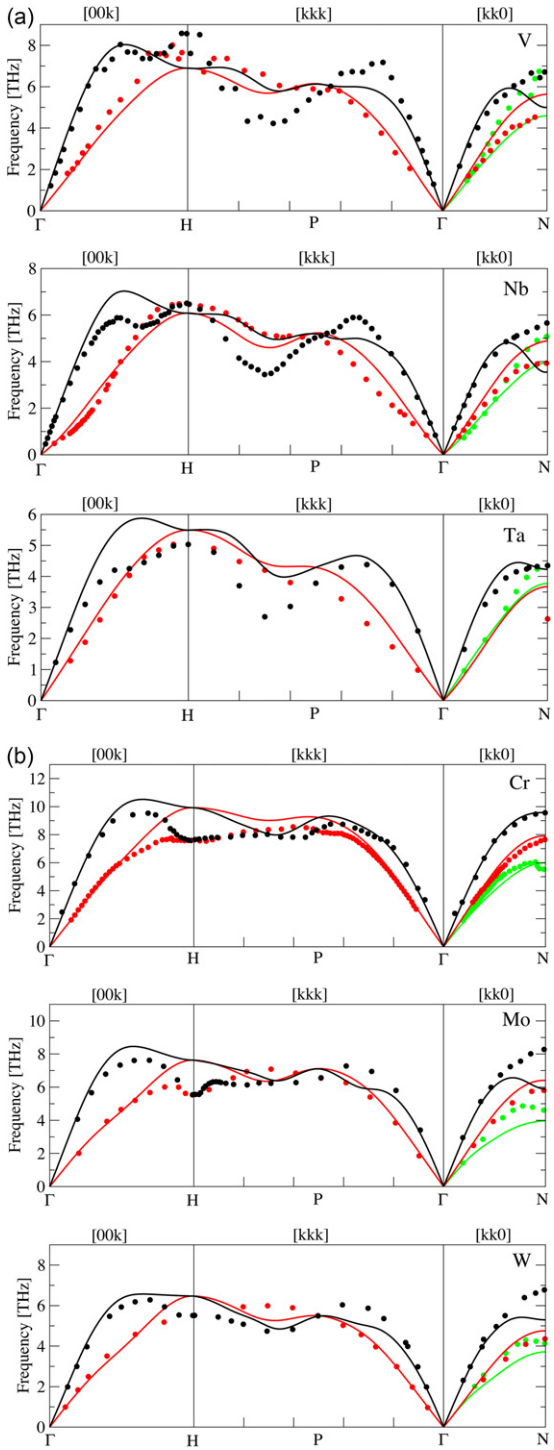

Figure 7. Phonon dispersion curves. Experimental data are from [74] for V, [75] for Nb, [76] for Ta, [77] for Cr, [78] for Mo and [79] for W. (*a*) Group V metals. (*b*) Group VI metals.

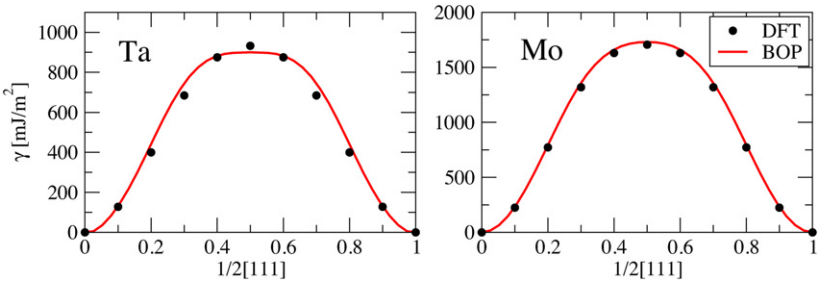

Figure 8. [1 1 1] cross sections of the unrelaxed γ-surfaces for the $(\bar{1}\,0\,1)$ plane in Ta and Mo.

figure 8 we show the [1 1 1] cross sections of the $(\bar{1}\,0\,1)$ γ-surfaces for Ta and Mo calculated using the constructed BOPs and compared with results of DFT calculations presented in [83]; for all the other metals studied, the results of γ-surface calculations are very similar. Since no relaxation was carried out in [83], the BOP calculations of γ-surfaces, shown in figure 8, were also made without any relaxation. In addition, we performed calculations with full relaxation perpendicular to the $(\bar{1}\,0\,1)$ plane using the developed BOPs. While the overall shape of the γ-surfaces does not change with relaxation, the values of the energy decrease by about 5–15%, depending on the element considered.

It can be seen in figure 8 that the γ-surfaces calculated using BOPs have not only the same functional form as those found in [83] using DFT, but the two calculations are even numerically very close. Importantly, as found in any previous studies of γ-surfaces [73], no metastable stacking faults are found, which is one of most important characteristics of all bcc metals [18].

However, γ-surfaces contain another piece of important information about the core of the $1/2[1\,1\,1]$ screw dislocation. As shown in many previous studies, the core of this dislocation is spread into the three $\{1\,0\,1\}$ planes of the [1 1 1] zone and there are two possible structures. Both of these two structures are invariant with respect to the [1 1 1] three-fold screw axis, but one of them is also invariant with respect to the $[1\,0\,\bar{1}]$ diad (reflection in the (1 1 1) plane followed by reflection in the $(1\,\bar{2}\,1)$plane) while the other is not and, consequently, another energetically equivalent configuration related by the $[1\,0\,\bar{1}]$ diad exists. The former structure is called non-degenerate and the latter degenerate; for details, see [18]. It was noted by Duesbery and Vitek [86] that the non-degenerate core can be regarded as containing six planar faults with the displacement 1/12[1 1 1] while the degenerate core as containing three planar faults with the displacement 1/6[1 1 1]. Hence, an approximate estimate of which of the core configurations is favoured may be performed using the γ-surface for the $\{1\,0\,1\}$ planes by comparing the total energies of the planar faults involved [86]. Specifically, the non-degenerate core is favoured if $2\gamma(1/12[1\,1\,1])/\gamma(1/6[1\,1\,1]) < 1$ and vice versa for the degenerate core. Table 8 gives the ratios $2\gamma(1/12[1\,1\,1])/\gamma(1/6[1\,1\,1])$ found when using the constructed BOPs for both relaxed and unrelaxed γ-surfaces. Since these ratios are smaller than the one for all of the metals studied, the core of the $1/2[1\,1\,1]$ screw dislocation is predicted to be non-degenerate in all non-magnetic bcc transition metals. Indeed, preliminary studies of the core of the $1/2[1\,1\,1]$ screw dislocation made using the constructed BOPs all show non-degenerate cores. The same cores were found in previous DFT-based studies [81–83, 85], as well as in calculations employing potentials developed on first-principles generalized pseudopotential theory in which the electronic structure is also treated fully quantum mechanically [87–90]. In contrast, a degenerate core has often been found when employing empirical, in particular central force potentials (see the review in [18]).

Table 8. Ratio of energies of the faults involved in non-degenerate and degenerate cores of $1/2\langle 1\,1\,1\rangle$ screw dislocations, respectively.

$2\gamma(1/12[1\,1\,1])/\gamma(1/6[1\,1\,1])$	V	Nb	Ta	Cr	Mo	W
BOP (unrelaxed)	0.80	0.76	0.82	0.84	0.79	0.78
BOP (relaxed)	0.82	0.79	0.86	0.84	0.90	0.87

5. Conclusions

In this paper, we have presented a new development in numerical bond-order potentials (BOPs) for the non-magnetic transition metals of groups V and VI. The basic principles on which the BOPs are founded are the same as in earlier developments [1] and the Oxford order-N package (OXON) is used in all of the calculations. This code, which is needed when using the BOPs, can be obtained from the authors upon request. The following are the two novel developments. First, in the attractive part of the cohesive energy, the bond integrals are based on the recently advanced method of the parametrization of tight-binding from DFT calculations [2, 3]. These integrals do not require any of the self-consistent screening that was necessary in previous developments [23, 25, 44]. When using these bond integrals, the computing time is significantly decreased compared with the previous version. Second, the empirical environment-dependent part of the repulsion has the same functional form as the repulsion arising from the overlap of the s and p electrons in solid argon in which no covalent bonding exists. The form of this dependence was proposed in [4] based on the tight-binding study of the energetics of solid argon subject to large pressures. This part of the repulsion, which captures the Cauchy pressure, is then supplemented by a pairwise potential that is repulsive at small separations of atoms and simultaneously provides a weak attraction at separations at or beyond the second nearest neighbours that arises from the interaction of s electrons and sd hybridization.

The testing of the developed BOPs was carried out by comparing calculations employing these potentials with DFT calculations and available experimental data. This study involved an investigation of the alternative higher energy structures and transformation paths connecting the bcc structure with the fcc, sc, hcp and bct structures via continuously distorted configurations. The agreement between the BOP and DFT calculations is excellent in both cases. The vacancy formation energies calculated using BOPs agree well with both the DFT calculations and experiments. Furthermore, satisfactory agreement with experimentally measured phonon dispersions for branches along the [1 0 0], [1 1 1] and [1 1 0] directions was found when using the developed BOPs. Finally, γ-surfaces calculated using BOPs agree closely with those determined by DFT calculations in [76] and they all suggest that the core of the $1/2\langle 1\,1\,1\rangle$ screw dislocations is always non-degenerate in non-magnetic transition metals. This is in full agreement with the available calculations that account fully for the quantum-mechanical nature of the bonding by d electrons, which provides the bulk of bonding in transition metals [81–83, 85, 87–90].

In summary, the testing of the constructed BOPs assures that they are transferable to structures well outside the regime of the ideal bcc lattice, the properties of which were used when fitting potential parameters. This is essential for the use of BOPs in studies involving crystal defects that govern various material properties. Hence, the developed BOPs can be applied with confidence when investigating the atomic structure and atomic level behaviour of extended crystal defects, such as dislocations, grain boundaries and other planar faults. Moreover, both the bond part of the energy that does not require any screening of bond

integrals as well as the new repulsive form can be employed in analytical BOPs that are being developed [91, 92].

Acknowledgments

We are grateful to Professor D G Pettifor, Professor R Drautz and Dr D Nguyen-Manh, Professor B Meyer and Dr M Reese for very fruitful discussions. During this research, YSL and VV were supported by the US Department of Energy, Office of Basic Energy Sciences, Grant No DEPG02-98ER45702 and MM by German Research Foundation (DFG), Grant No MR 22/5-1 and by the European Commission, Contract No NMP.2010.2.5-1.263335 (MultiHy).

References

[1] Aoki M, NguyenManh D, Pettifor D G and Vitek V 2007 *Prog. Mater. Sci.* **52** 154
[2] Madsen G K H, McEniry E J and Drautz R 2011 *Phys. Rev.* B **83** 4119
[3] Urban A, Reese M, Mrovec M, Elsässer C and Meyer B 2011 *Phys. Rev.* B **84** 155119
[4] Aoki M and Kurokawa T 2007 *J. Phys.: Condens. Matter* **19** 136228
[5] Finnis M W 2003 *Interatomic Forces in Condensed Matter* (Oxford: Oxford University Press)
[6] Sholl D S and Steckel J A 2009 *Density Functional Theory: A Practical Introduction* (Hoboken, NJ: Wiley)
[7] Dreizler R M and Gross E K U 2013 *Density Functional Theory* (Berlin: Springer)
[8] Pettifor D G 1997 *Phys. Educ.* **32** 164
[9] Daw M S and Baskes M I 1984 *Phys. Rev.* B **29** 6443
[10] Finnis M W and Sinclair J E 1984 *Phil. Mag.* A **50** 45
[11] Ackland G J and Thetford R 1987 *Phil. Mag.* A **56** 15
[12] Mendelev M I, Han S, Srolovitz D J, Ackland G J, Sun D Y and Asta M 2003 *Phil. Mag.* **83** 3977
[13] Derlet P M, NguyenManh D and Dudarev S L 2007 *Phys. Rev.* B **76** 4107
[14] Fellinger M R, Park H and Wilkins J W 2010 *Phys. Rev.* B **81** 4119
[15] Gordon P A, Neeraj T and Mendelev M I 2011 *Phil. Mag.* **91** 3931
[16] Friedel J 1969 *The Physics of Metals* ed J M Ziman (Cambridge: Cambridge University Press) pp 340
[17] Pettifor D G 1995 *Bonding and Structure of Molecules and Solids* (Oxford: Oxford University Press)
[18] Vitek V and Paidar V 2008 *Dislocations in Solids* ed J P Hirth (Amsterdam: Elsevier) pp 439
[19] Mishin Y and Lozovoi A Y 2006 *Acta Mater.* **54** 5013
[20] Bercegeay C, Jomard G and Bernard S 2008 *Phys. Rev.* B **77** 4203
[21] Sutton A P 1993 *Electronic Structure of Materials* (Oxford: Oxford University Press)
[22] Pettifor D G 1989 *Phys. Rev. Lett.* **63** 2480
[23] Mrovec M, Nguyen-Manh D, Pettifor D G and Vitek V 2004 *Phys. Rev.* B **6909** 4115
[24] Cawkwell M J, NguyenManh D, Pettifor D G and Vitek V 2006 *Phys. Rev.* B **7306** 4104
[25] Mrovec M, Gröger R, Bailey A G, Nguyen-Manh D, Elsässer C and Vitek V 2007 *Phys. Rev.* B **7510** 4119
[26] Gröger R, Bailey A G and Vitek V 2008 *Acta Mater.* **56** 5401
[27] Finnis M W 2007 *Prog. Mater. Sci.* **52** 133
[28] Hammerschmidt T, Drautz R and Pettifor D G 2009 *Int. J. Mater. Res.* **100** 1479
[29] Hammerschmidt T and Drautz R 2009 *Multiscale Simulation Methods in Molecular Sciences* ed J Grotendorst *et al* (Jülich: Institute for Advanced Simulation, Forschungszentrum Jülich, NIC Series) pp 229
[30] Slater J C and Koster G F 1954 *Phys. Rev.* **94** 1498
[31] Aoki M 1993 *Phys. Rev. Lett.* **71** 3842
[32] Aoki M and Pettifor D G 1994 *Mater. Sci. Eng.* A **176** 19
[33] Lanczos C 1950 *J. Res. Natl Bur. Stand.* **45** 225

[34] Aoki M and Pettifor D G 1993 *Int. J. Mod. Phys.* B **7** 299
[35] Mrovec M, Nguyen-Manh D, Elsässer C and Gumbsch P 2011 *Phys. Rev. Lett.* **106** 6402
[36] Mermin N D 1965 *Phys. Rev.* A **137** 1441
[37] Bowler D R, Aoki M, Goringe C M, Horsfield A P and Pettifor D G 1997 *Modelling Simul. Mater. Sci. Eng.* **5** 199
[38] Girshick A, Bratkovsky A M, Pettifor D G and Vitek V 1998 *Philos. Mag.* A **77** 981
[39] Horsfield A P 1996 *Mater. Sci. Eng.* B **37** 219
[40] Horsfield A P and Bratkovsky A M 1996 *Phys. Rev.* B **53** 15381
[41] Horsfield A P, Bratkovsky A M, Fearn M, Pettifor D G and Aoki M 1996 *Phys. Rev.* B **53** 12694
[42] Horsfield A P, Bratkovsky A M, Pettifor D G and Aoki M 1996 *Phys. Rev.* B **53** 1656
[43] Nguyen-Manh D, Vitek V and Horsfield A P 2007 *Prog. Mater. Sci.* **52** 255
[44] Nguyen-Manh D, Pettifor D G and Vitek V 2000 *Phys. Rev. Lett.* **85** 4136
[45] Chadi D J 1984 *Phys. Rev.* B **29** 785
[46] Sutton A P, Finnis M W, Pettifor D G and Ohta Y 1988 *J. Phys. C: Solid State* **21** 35
[47] Sob M and Vitek V 1996 in Stability of Materials: NATO Advanced Science Institute ed. A Gonis *et al* (New York: Plenum) pp 449
[48] Nguyen-Manh D, Pettifor D G, Znam S and Vitek V 1998 *Tight-Binding Approach to Computational Materials Science* ed P E A Turchi *et al* (Pittsburgh: Materials Research Society) pp 353
[49] Marcus P M, Qiu S-L and Moruzzi V L 1998 *J. Phys: Condens. Matter* **10** 6541
[50] Paidar V, Wang L G, Sob M and Vitek V 1999 *Modelling Simul. Mater. Sci. Eng.* **7** 369
[51] Kana T, Sob M and Vitek V 2011 *Intermetallics* **19** 919
[52] Löwdin P-O 1950 *J. Chem. Phys.* **18** 365
[53] Goodwin L, Skinner A J and Pettifor D G 1989 *Europhys. Lett.* **9** 701
[54] Harris J 1985 *Phys. Rev.* B **31** 1770
[55] Foulkes W M C 1989 *Atomistic Simulations of Materials: Beyond Pair Potentials* ed V Vitek and D Srolovitz (New York: Plenum) pp 353
[56] Gröger R, Racherla V, Bassani J L and Vitek V 2008 *Acta Mater.* **56** 5412
[57] Gröger R and Vitek V 2008 *Acta Mater.* **56** 5426
[58] Cak M, Vitek V and Lin Y-S 2010 unpublished
[59] Pettifor D G 1978 *J. Phys. F: Metal Phys.* **8** 219
[60] Kresse G and Hafner J 1993 *Phys. Rev.* B **47** 558
[61] Kresse G and Furthmüller J 1996 *Phys. Rev.* B **54** 11169
[62] Kresse G and Furthmüler J 1996 *Comput. Mater. Sci.* **6** 15
[63] Hafner J 2007 *Comput. Phys. Commun.* **177** 6
[64] Kittel C 1996 *Introduction to Solid State Physics* 7th edn (New York: Wiley)
[65] Bujard P 1982 *Elastic constants of BCC metals* (Geneva: University of Geneva)
[66] Vitek V 1968 *Phil. Mag.* A **18** 773
[67] Kresse G and Hafner J 1994 *Phys. Rev.* B **49** 14251
[68] Haas H, Wang C Z, Fähnle M, Elsässer C and Ho K M 1998 *Phys. Rev.* B **57** 1461
[69] Ullmaier 1991 *Landolt–Börstein Numerical Data and Functional Relationships in Science and Technology, Group III* (Berlin: Springer)
[70] Nguyen-Manh D, Horsfield A P and Dudarev S L 2006 *Phys. Rev.* B **73** 020101(R)
[71] Bain E C 1924 *Trans. AIME* **70** 25
[72] Kunc K 1985 *Electronic Structure Dynamics and Quantum Structure Properties of Condensed Matter* (New York: Plenum)
[73] Finnis M W, Kear K L and Pettifor D G 1984 *Phys. Rev. Lett.* **52** 291
[74] Colella R and Batterman B 1970 *Phys. Rev.* B **1** 3913
[75] Nakagawa Y and Woods A 1963 *Phys. Rev. Lett.* **11** 271
[76] Woods A D B 1964 *Phys. Rev.* **136** A781
[77] Shaw W and Muhlestein L 1971 *Phys. Rev.* B **4** 969
[78] Woods A D B and Chen S H 1964 *Solid State Commun.* **2** 233
[79] Chen S H and Brockhouse B N 1964 *Solid State Commun.* **2** 73
[80] Duesbery M S 1989 *Dislocations in Solids* ed F R N Nabarro (Amsterdam: Elsevier) pp 67

[81] Woodward C and Rao S I 2001 *Phil. Mag.* A **81** 1305
[82] Woodward C and Rao S I 2002 *Phys. Rev. Lett.* **8821** 6402
[83] Frederiksen S L and Jacobsen K W 2003 *Phil. Mag.* **83** 365
[84] Itakura M, Kaburaki H and Yamaguchi M 2012 *Acta Mater.* **60** 3698
[85] Weinberger C R, Tucker G J and Foiles S M 2013 *Phys. Rev.* B **87** 054114
[86] Duesbery M S and Vitek V 1998 *Acta Mater.* **46** 1481
[87] Moriarty J A 1990 *Many-Atom Interactions in Solids* ed R M Nieminen *et al* (Berlin: Springer) pp 158
[88] Xu W and Moriarty J A 1996 *Phys. Rev.* B **54** 6941
[89] Yang L H, Soderlind P and Moriarty J A 2001 *Phil. Mag.* A **81** 1355
[90] Moriarty J A, Vitek V, Bulatov V V and Yip S 2002 *J. Comput.-Aided Mater. Des.* **9** 99
[91] Cak M, Hammerschmidt T and Drautz R 2013 *J. Phys.: Conden. Matter* **25** 265002
[92] Seiser B, Pettifor D G and Drautz R 2013 *Phys. Rev.* B **87** 094105